Catalytic domain of MMP20 (Enamelysin) – The NMR structure of a new matrix metalloproteinase

Yvonne Arendt[a], Lucia Banci[a,b], Ivano Bertini[a,b,*], Francesca Cantini[b], Roberta Cozzi[b], Rebecca Del Conte[a,b], Leonardo Gonnelli[a,b]

[a] *ProtEra S.r.l., Via delle Idee 22, 50019 Sesto Fiorentino (FI), Italy*
[b] *Magnetic Resonance Center (CERM), University of Florence, Via L. Sacconi 6, 50019 Sesto Fiorentino, Italy*

Abstract The solution structure of the catalytic domain of MMP-20, a member of the matrix metalloproteinases family not yet structurally characterized, complexed with *N*-Isobutyl-*N*-(4-methoxyphenylsulfonyl)glycyl hydroxamic acid (NNGH), is here reported and compared with other MMPs–NNGH adducts. The backbone dynamic has been characterized as well. We have found that, despite the same fold and very high overall similarity, the present structure experiences specific structural and dynamical similarities with some MMPs and differences with others, around the catalytic cavity. The present solution structure, not only contributes to fill the gap of structural knowledge on human MMPs, but also provides further information to design more selective and efficient inhibitors for a specific member of this class of proteins.
© 2007 Federation of European Biochemical Societies. Published by Elsevier B.V. All rights reserved.

Keywords: NMR; Solution structure; Protein–ligand interaction; MMP

1. Introduction

The knowledge of the structure of a target is a prerequisite to design and optimize efficient and selective drugs, particularly when selectivity regards a family of targets.

Matrix metalloproteinases (MMPs) are a family of enzymes belonging to the class of zinc- and calcium-dependent endopeptidases, involved in extracellular matrix degradation or remodeling [1,2]. Overexpression or misregulation of MMPs is related to several pathologies [3,4], and therefore their inhibition is relevant in drug discovery [5].

MMPs are multidomains enzymes, constituted at least by a prodomain and a catalytic domain. The latter contains two zinc(II) ions, one catalytic and the other, together with one to three calcium(II) ions, with a structural role [6]. The substrate/inhibitor penetrates in a hydrophobic S1' pocket of the catalytic domain whose size is variable within the MMPs family and affects the substrate/inhibitor specificity for a given MMP [5–7]. Human MMPs are 23 and a number of structures of the catalytic domain complexed with a variety of inhibitors, is known [6–10]. Still, there are members of the family poorly characterized

[11,12]. Enamelysin (MMP-20) is one among these; it is expressed exclusively in tooth-forming cells with an essential role in normal dental enamel development [13]. *MMP20*-null mice displays multiple enamel defects and mutations of the human *MMP20* gene have been associated with autosomal recessive types of *amelogenesis imperfecta* [14], indicating that MMP-20 is a critical molecule for tooth enamel formation.

We report here the first structure determination and mobility studies of the catalytic domain of MMP-20 complexed with a non-peptidic inhibitor (NNGH). The solution structure and the dynamic data are then compared with those of other MMPs complexed with the same inhibitor.

2. Materials and methods

2.1. Sample preparation

The gene codifying the catalytic domain of MMP-20 (aa 113–272) was cloned, expressed, and purified following an already reported protocol [8]. The MMP-20–NNGH adduct was prepared by adding the NNGH during the final concentration step. The NMR protein sample concentration, determined by UV spectroscopy (extinction coefficient of $2.84 \times 10^4 \, M^{-1} \, cm^{-1}$ at 280 nm), are 1.0–1.4 mM in Tris 20 mM, pH 8, $ZnCl_2$ 0.1 mM, $CaCl_2$ 5 mM, NaCl 300 mM and acetohydroxamic acid 0.3 M. Two equivalents of Ca^{2+} per protein were found from inductively coupled plasma emission spectroscopy measurements.

The inhibition constant was determined, in terms of dissociation constant Kd, evaluating the ability of NNGH to prevent hydrolysis of the peptide Mca-Pro-Leu-Gly-Leu-Dpa-Ala-Arg-NH2, from the initial hydrolysis reaction velocities at a fixed concentration of enzyme [15]. These measurements were performed in 50 mM HEPES buffer, with 10 mM $CaCl_2$, 0.05% Brij-35, 0.1 mM $ZnCl_2$ (pH 7.0), with non-saturating substrate concentrations.

2.2. NMR experiments and structure calculations of MMP-20–NNGH complex

The NMR experiments performed on the MMP-20–NNGH complex are reported in Table S1 of the Supplementary material, resonances assignment in Table S2 and deposited in the BioMagResBank. The His coordination mode to the two zinc ions and the nature of the coordinating nitrogens was determined through ^1H–^{15}N heteronuclear experiment to detect ^2J ^1H–^{15}N couplings between the imidazole nitrogen and non-exchangeable imidazole protons [16]. Each of the 20 lowest target function conformers was energy-minimized in explicit solvent with the program AMBER-8 [17]. Table S3 reports statistics on restraint violations in the final structure together with selected quality parameters [18–20].

The R_1 and R_2 relaxation rates [21], and ^1H–^{15}N NOEs values [22] were measured at 600 MHz (298 K) (Fig. S1). R_2 was also measured as a function of the refocusing time (τ_{CPMG}) in a Carr–Purcell–Meiboom–Gill (CPMG) sequence [23], which ranged between 450 and 1150 µs. The R_1 and R_2 relaxation rates and ^1H–^{15}N NOEs have average values of $1.42 \pm 0.16 \, s^{-1}$, $14.0 \pm 1.6 \, s^{-1}$ and 0.80 ± 0.11,

*Corresponding author. Address: Magnetic Resonance Center, University of Florence, Via L. Sacconi 6, 50019 Sesto Fiorentino, Italy. Fax: +39 055 4574273.
E-mail address: ivanobertini@cerm.unifi.it (I. Bertini).

respectively. A correlation time for protein tumbling (τ_c) of 9.5 ± 0.1 ns was obtained from the R_2/R_1 ratio, consistent with the molecular weight of the catalytic domain of MMP-20 being in the monomeric state and with the value predicted by using HYDRONMR program [24]. The relaxation data were analyzed with the program TENSOR2 [25] which follows the model-free approach of Lipari and Szabo [26] (Fig. S2).

A ^{15}N labeled MMP-20–NNGH sample was dialyzed against D$_2$O buffer to perform the H$_2$O/D$_2$O exchange experiments. Then, a ^{1}H–^{15}N HSQC spectrum of the sample was recorded after three days.

3. Results and discussion

3.1. Solution structure of the MMP-20–NNGH complex

The catalytic domain of MMP-20 shares high sequence similarity with other MMPs, from a minimum of 36% with MMP-21 to a maximum of 60% with MMP-13 and MMP-2 [27]. Accordingly, the solution structure of the catalytic domain of MMP-20–NNGH adduct shows the typical fold common to all MMP catalytic domains (Fig. 1) [7], which consists of three α-helices and a twisted five stranded β-sheet with a further short two-stranded β-sheet located in the C-terminal part of loop 7. The structure is overall stabilized by multiple hydrophobic interactions and by a network of H-bonds directly identified through H$_2$O/D$_2$O exchange experiments. The secondary structure elements are well ordered (RMSD value within the family of 0.41 ± 0.06 Å) and only a few residues in the loops (4, 5, 7 and 8) are slightly more disordered (Fig. S3). Consistently, the order parameters S^2, which monitor motions in the ns–ps range are almost homogenous over the entire protein except for few residues located in loops (Fig. S2). However, internal dynamics is limited also in the loops and, in particular, in the active-site loop (loop 8) which, on the contrary, is highly dynamic in several other MMPs previously characterized, as MMP-1 [28], MMP-3 [10], MMP-12 [29] and MMP-13 [30]. The amplitudes of the backbone motions change from MMP3–NNGH with an average S^2 value of 0.85 ± 0.05 [29], to MMP-20–NNGH with S^2 of 0.94 ± 0.04. This trend is also observed in the active-site region, where a number of MMP-20 residues have S^2 values higher than 0.90 and higher then in MMP-3 (Fig. S4). Some residues, all located in loops, are involved in exchange processes occurring in the
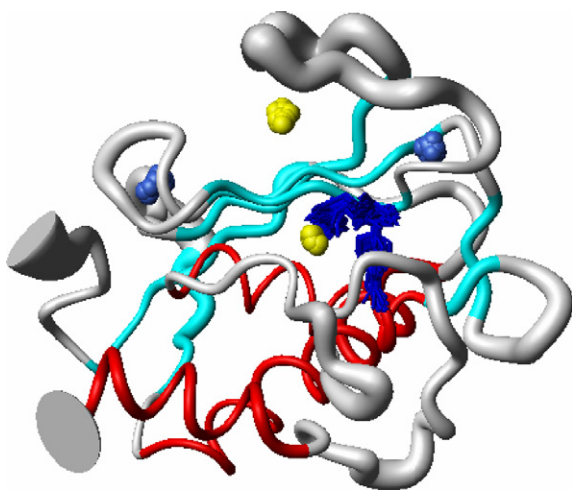

Fig. 1. Solution structure of the catalytic domain of the MMP-20–NNGH adduct. The zinc and calcium ions are in yellow and light blue, respectively. The NNGH is in blue.

ms–μs time range (Fig. S2). The occurrence of both conformational exchange processes and ns–ps motions for some residues belonging to loop 5 matches the paucity of NOEs for this loop (Fig. S3-A), and consequently is higher structural disorder (Fig S3-B).

The two zinc and the two calcium ions have the same ligands as found in other MMPs [27]. As suggested from sequence analysis [27], the third calcium site is not conserved in MMP-20 as experimentally confirmed by inductively coupled plasma emission.

The binding mode of the NNGH inhibitor, which is similar to that reported for other MMPs [8,10,29], is well defined by 61 intermolecular NOEs (Table S4). Its phenyl group penetrates into the S1′ pocket establishing hydrophobic contacts, with residues located in four distinct regions: Val223, His226 and Glu227 in helix α2, Ala190 and His191 in strand β4, Thr188, Leu189 in loop 5 and His236, Leu243, Thr247 and Tyr248 in loop 8. These regions define the S1′ and S2′ pockets of MMP-20. The latter pocket is shallow and accommodates the isobutyl side chain of NNGH, which is essentially solvent exposed (Table S4). NNGH is also stabilized by H-bonds with protein residues.

3.2. Comparison of the solution structure of MMP-20–NNGH with other MMP–NNGH complexes

The structures of MMP-3-, MMP-10- and MMP-12–NNGH adducts (2JNP, 1Q3A, 1RMZ) are very close to that of MMP-20–NNGH, with an average RMSD of 1.7 Å (Fig. 2A). Structural variations, outside the uncertainty of the structures, are located in loop regions, in particular in loops 5, 7 and 8. The hydroxamate group and the pattern of H-bonds is also the same for all four structures. Also sequence similarity with these proteins is very high (Table S5). From the sequence analysis (Fig. 2B) it appears that about 20 residues are the same or have very similar chemical properties in MMP-3 and MMP-10 but have a different nature in both MMP-20 and MMP-12, being identical or similar in these latter two proteins. These amino acid variations could explain the similar inhibition constants for NNGH of MMP-20 and MMP-12 on one side (17 nM and 13 nM [29], respectively), with respect to those of MMP-3 and MMP-10 on the other (130 nM [31] and 100 nM [8]).

Contacts within 5 Å between NNGH and these proteins involve residues located in strand β4, helix α2, loops 5 and 8. The major differences in the sequence among these four MMPs are mainly located in the last region, where structural differences are observed (Fig. 2B). They contribute to determine different shape and size of the S1' cavity in MMP-20 and MMP-12 with respect to MMP-10 and MMP-3, being in the latter two more open than in MMP-20 and MMP-12. In MMP-10 and MMP-3 a Ser and a Thr, located in positions 249 and 251, respectively, on loop 8 (MMP-20 numbering), are oriented towards loop 7 and solvent exposed, determining a more open conformation of loop 8. On the contrary, in MMP-20 and MMP-12 the residue in position 251 (Lys and Val, respectively) is pointing toward loop 8 and extends into the S1′ pocket (Fig. 2A), while a one-residue gap is present in position 249 (Fig. 2B). The structural differences around the catalytic cavity between the two pairs of proteins could play a role in determining their pairwise different K_d values for NNGH.

Structural and mutagenesis studies indicated that residues in the S1' pocket, and particularly in position 222 (MMP-20 numbering) have a role in shaping this pocket [6]. A Leu is
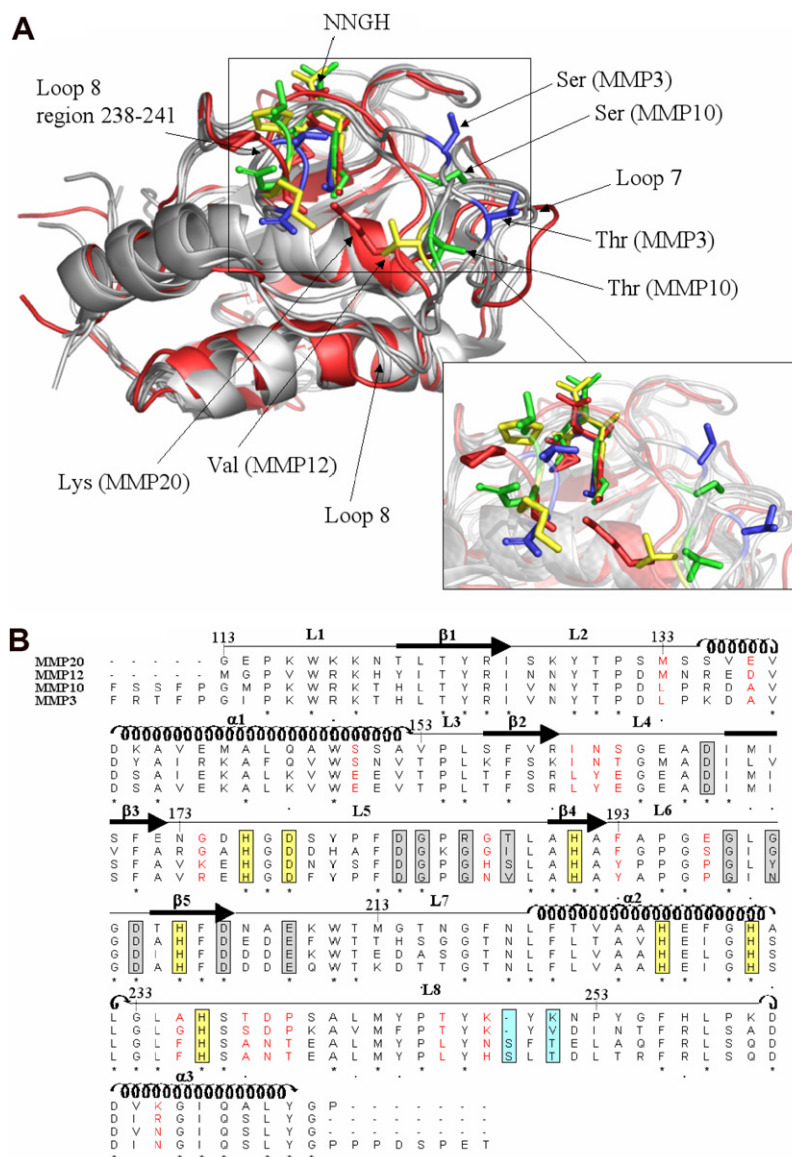
Fig. 2. (A) Catalytic domain of the MMP-20–NNGH adduct (red) superimposed with MMP-12-, MMP-10- and MMP-3–NNGH. Relevant residues defining the S1′ pocket are also shown in yellow, green and blue for MMP-12, MMP-10 and MMP-3, respectively. (B) Sequence alignment of MMP-20, MMP-12, MMP-10 and MMP-3 proteins. The residues coordinating the catalytic and the structural zinc ions are in yellow boxes, those binding the calcium ions are in gray boxes. Residues in position 249 and 251 (MMP-20 numbering) are in cyan boxes. Residues having similar chemical properties in MMP-10 and MMP-3 but different in both MMP-20 and MMP-12 are colored in red.

usually present (Fig. 2B), or less often an Arg residue. MMP-20 is the only one to have a Thr in this position. The side chain of this residue is oriented towards the methoxy group of the inhibitor in all the MMP–NNGH available structures forming protein-inhibitor/substrate interactions. Also this residue could be therefore important in regulating the MMP-20 substrate specificity considering the different steric hindrance between a Leu and a Thr.

4. Concluding remarks

The structure of another member of the MMPs family is here reported for the first time, thus contributing to fill the gap of structural knowledge on this important class of drug targets. Despite the overall similarity in structure within the proteins of the family, knowledge of the subtle structural dif-

ferences among MMPs could contribute to the design of more efficient and selective inhibitors within MMPs family [32,33]. The relevance of selectivity is increased by the need to avoid the inhibition of MMP-20, since deletion of MMP-20 gene or its mutation are associated to pathologic states [14].

Appendix A. Supplementary data

The atomic coordinates and structural restraints for MMP-20–NNGH have been deposited in Protein Data Bank and

BMRB (code ID: 2JSD and 15361, respectively). Supplementary data associated with this article can be found, in the online version, at doi:10.1016/j.febslet.2007.08.069.

References

[1] Woessner Jr., J.F. and Nagase, H. (1999) Matrix metalloproteinases. J. Biol. Chem. 274, 21491–21494.

[2] Birkedal-Hansen, H., Moore, W.G., Bodden, M.K., Windsor, L.J., Birkedal-Hansen, B., DeCarlo, A. and Engler, J.A. (1993) Matrix metalloproteinases: a review. Crit. Rev. Oral Biol. Med. 4, 197–250.

[3] MacDougall, J.R. and Matrisian, L.M. (1995) Contributions of tumor and stromal matrix metalloproteinases to tumor progression, invasion and metastasis. Cancer Metast. Rev. 14, 351–362.

[4] Shapiro, S.D. (1998) Matrix metalloproteinase degradation of extracellular matrix: biological consequences. Curr. Opin. Cell Biol. 10, 602–608.

[5] Fisher, J.F. and Mobashery, S. (2006) Recent advances in MMP inhibitor design. Cancer Metast. Rev. 25, 115–136.

[6] Bode, W., Fernandez-Catalan, C., Tschesche, H., Grams, F., Nagase, H. and Maskos, K. (1999) Structural properties of matrix metalloproteinases. Cell Mol. Life Sci. 55, 639–652.

[7] Maskos, K. (2005) Crystal structures of MMPs in complex with physiological and pharmacological inhibitors. Biochimie 87, 249–263.

[8] Bertini, I., Calderone, V., Fragai, M., Luchinat, C., Mangani, S. and Terni, B. (2004) Crystal structure of the catalytic domain of human matrix metalloproteinase 10. J. Mol. Biol. 336, 707–716.

[9] Bertini, I., Calderone, V., Fragai, M., Luchinat, C., Mangani, S. and Terni, B. (2003) X-ray structures of ternary enzyme-product-inhibitor complexes of MMP. Angew. Chem. Int. Ed. 42, 2673–2676.

[10] Alcaraz, L.A., Banci, L., Bertini, I., Cantini, F., Donaire, A. and Gonnelli, L. (2007) MMP-inhibitor interaction: the solution structure of the catalytic domain of human matrix metalloproteinase-3 with three inhibitors. J. Biol. Inorg. Chem.

[11] Uria, J.A. and Lopez-Otin, C. (2000) Matrilysin-2, a new matrix metalloproteinase expressed in human tumors and showing the minimal domain organization required for secretion, latency, and activity. Cancer Res. 60, 4745–4751.

[12] Llano, E., Pendas, A.M., Knauper, V., Sorsa, T., Salo, T., Salido, E., Murphy, G., Simmer, J.P., Bartlett, J.D. and Lopez-Otin, C. (1997) Identification and structural and functional characterization of human Enamelysin (MMP-20). Biochemistry 36, 15101–15108.

[13] Turk, B.E., Lee, D.H., Yamakoshi, Y., Klingenhoff, A., Reichenberger, E., Wright, J.T., Simmer, J.P., Komisarof, J.A., Cantley, L.C. and Bartlett, J.D. (2006) MMP-20 is predominately a tooth-specific enzyme with a deep catalytic pocket that hydrolyzes type V collagen. Biochemistry 45, 3863–3874.

[14] Ozdemir, D., Hart, P.S., Ryu, O.H., Choi, S.J., Ozdemir-Karatas, M., Firatli, E., Piesco, N. and Hart, T.C. (2005) MMP20 active-site mutation in hypomaturation amelogenesis imperfecta. J. Dent. Res. 84, 1031–1035.

[15] Kuzmic, P., Elrod, K.C., Cregar, L.M., Sideris, S., Rai, R. and Janc, J.W. (2000) High-throughput screening of enzyme inhibitors: simultaneous determination of tight-binding inhibition constants and enzyme concentration. Anal. Biochem. 286, 45–50.

[16] Banci, L., Benedetto, M., Bertini, I., Del Conte, R., Piccioli, M. and Viezzoli, M.S. (1998) Solution structure of reduced monomeric Q133M2 copper, zinc superoxide dismutase. Why is SOD a dimeric enzyme? Biochemistry 37, 11780–11791.

[17] Case, D.A., Darden, T.A., Cheatham, T.E., Simmerling, C.L., Wang, J., Duke, R.E., Luo, R., Merz, K.M., Wang, B., Pearlman, D.A., Crowley, M., Brozell, S., Tsui, V., Gohlke, H., Mongan, J.,

[18] Hornak, V., Cui, G., Beroza, P., Schafmeister, C.E., Caldwell, J.W., Ross, W.S., and Kollman, P.A. AMBER 8. [8.0]. 2004. San Francisco, CA, University of California.

[18] Laskowski, R.A., Rullmann, J.A.C., MacArthur, M.W., Kaptein, R. and Thornton, J.M. (1996) AQUA and PROCHECK-NMR: programs for checking the quality of protein structures solved by NMR. J. Biomol. NMR 8, 477–486.

[19] Vriend, G. (1990) WHAT IF: a molecular modeling and drug design program. J. Mol. Graphics 8, 52–56.

[20] Nabuurs, S.B., Spronk, C.A., Krieger, E., Maassen, H., Vriend, G. and Vuister, G.W. (2003) Quantitative evaluation of experimental NMR restraints. J. Am. Chem. Soc. 125, 12026–12034.

[21] Farrow, N.A., Muhandiram, R., Singer, A.U., Pascal, S.M., Kay, C.M., Gish, G., Shoelson, S.E., Pawson, T., Forman-Kay, J.D. and Kay, L.E. (1994) Backbone dynamics of a free and phosphopeptide-complexed Src homology 2 domain studied by 15N NMR relaxation. Biochemistry 33, 5984–6003.

[22] Grzesiek, S. and Bax, A. (1993) The importance of not saturating H_2O in protein NMR. Application to sensitivity enhancement and NOE measurements. J. Am. Chem. Soc. 115, 12593–12594.

[23] Orekhov, V.Yu., Pervushin, K.V. and Arseniev, A.S. (1994) Backbone dynamics of (1–71) bacterioopsin studied by two-dimensional ^1H–^{15}N NMR spectroscopy. Eur J Biochem. 219, 887–896.

[24] Garcia, D.L.T., Huertas, M.L. and Carrasco, B. (2000) HYDRONMR: prediction of NMR relaxation of globular proteins from atomic-level structures and hydrodynamic calculations. J. Magn. Reson. 147, 138–146.

[25] Dosset, P., Hus, J.C., Blackledge, M. and Marion, D. (2000) Efficient analysis of macromolecular rotational diffusion from heteronuclear relaxation data. J. Biomol. NMR 16, 23–28.

[26] Lipari, G. and Szabo, A. (1982) Model-free approach to the interpretation of nuclear magnetic resonance relaxation in macromolecules. 2. Analysis of experimental results. J. Am. Chem. Soc. 104, 4559–4570.

[27] Andreini, C., Banci, L., Bertini, I., Luchinat, C. and Rosato, A. (2004) A bioinformatic comparison of structures and homology-models of matrix metalloproteinases. J. Proteome Res. 3, 21–31.

[28] Moy, F.J., Chanda, P.K., Chen, J.M., Cosmi, S., Edris, W., Skotnicki, J.S., Wilhelm, J. and Powers, R. (1999) NMR solution structure of the catalytic fragment of human fibroblast collagenase complexed with a sulfonamide derivative of a hydroxamic acid compound. Biochemistry 38, 7085–7096.

[29] Bertini, I., Calderone, V., Cosenza, M., Fragai, M., Lee, Y.-M., Luchinat, C., Mangani, S., Terni, B. and Turano, P. (2005) Conformational variability of MMPs: beyond a single 3D structure. Proc. Natl. Acad. Sci. USA 102, 5334–5339.

[30] Zhang, X., Gonnella, N.C., Koehn, J., Pathak, N., Ganu, V., Melton, R., Parker, D., Hu, S. and Nam, K.Y. (2000) Solution Structure of the catalytic domain of human collagenase-3 (MMP-13) complexed to a potent non-peptidic sulfonamide inhibitor:binding comparison with stromelysin-1 and collagenase-1. J. Mol. Biol. 301, 513–524.

[31] MacPherson, L.J., Bayburt, E.K., Capparelli, M.P., Carroll, B.J., Goldstein, R., Justice, M.R., Zhu, L., Hu, S., Melton, R.A., Fryer, L., Goldberg, R.L., Doughty, J.R., Spirito, S., Blancuzzi, V., Wilson, D., O'Byrne, E.M., Ganu, V. and Parker, D.T. (1997) Discovery of CGS 27023A, a non-peptidic, potent, and orally active stromelysin inhibitor that blocks cartilage degradation in rabbits. J. Med. Chem. 40, 2525–2532.

[32] Bertini, I., Calderone, V., Fragai, M., Giachetti, A., Loconte, M., Luchinat, C., Maletta, M., Nativi, C. and Yeo, K.J. (2007) Exploring the subtleties of drug–receptor interactions: the case of matrix metalloproteinases. J. Am. Chem. Soc. 129, 2466–2475.

[33] Cuniasse, P., Devel, L., Makaritis, A., Beau, F., Georgiadis, D., Matziari, M., Yiotakis, A. and Dive, V. (2005) Future challenges facing the development of specific active-site-directed synthetic inhibitors of MMPs. Biochimie 87, 393–402.